


Laser monitoring of dynamic behavior of magnetic nanoparticles in magnetic field gradient

Cite as: AIP Advances **10**, 015025 (2020); <https://doi.org/10.1063/1.5130167>

Submitted: 03 October 2019 . Accepted: 11 December 2019 . Published Online: 10 January 2020

Kenta Tsunashima , Katsuya Jinno , Bunta Hiramatsu, Kayo Fujimoto, Kenji Sakai, Toshihiko Kiwa, Mohd Mawardi Saari, and Keiji Tsukada

COLLECTIONS

Paper published as part of the special topic on [64th Annual Conference on Magnetism and Magnetic Materials](#), [Chemical Physics](#), [Energy, Fluids and Plasmas](#), [Materials Science](#) and [Mathematical Physics](#)

Note: This paper was presented at the 64th Annual Conference on Magnetism and Magnetic Materials.



View Online



Export Citation



CrossMark

ARTICLES YOU MAY BE INTERESTED IN

[Magnetic characterization change by solvents of magnetic nanoparticles in liquid-phase magnetic immunoassay](#)

AIP Advances **9**, 125317 (2019); <https://doi.org/10.1063/1.5130168>

[Exchange bias in \$\text{La}_{0.7}\text{Sr}_{0.3}\text{CrO}_3/\text{La}_{0.7}\text{Sr}_{0.3}\text{MnO}_3/\text{La}_{0.7}\text{Sr}_{0.3}\text{CrO}_3\$ heterostructures](#)

AIP Advances **10**, 015001 (2020); <https://doi.org/10.1063/1.5130453>

[Second harmonic response of magnetic nanoparticles under parallel static field and perpendicular oscillating field for magnetic particle imaging](#)

AIP Advances **10**, 015007 (2020); <https://doi.org/10.1063/1.5129973>



NEW: TOPIC ALERTS

Explore the latest discoveries in your field of research

SIGN UP TODAY!

Laser monitoring of dynamic behavior of magnetic nanoparticles in magnetic field gradient

Cite as: AIP Advances 10, 015025 (2020); doi: 10.1063/1.5130167
Presented: 6 November 2019 • Submitted: 3 October 2019 •
Accepted: 11 December 2019 • Published Online: 10 January 2020



Kenta Tsunashima,^{1,a)}  Katsuya Jinno,¹  Bunta Hiramatsu,¹ Kayo Fujimoto,¹ Kenji Sakai,¹
Toshihiko Kiwa,¹ Mohd Mawardi Saari,² and Keiji Tsukada¹

AFFILIATIONS

¹Graduate School of Interdisciplinary Science and Engineering in Health Systems, Okayama University, Okayama 700-8530, Japan

²Faculty of Electrical & Electronic Engineering, Universiti Malaysia Pahang, 26600 Pekan, Pahang, Malaysia

Note: This paper was presented at the 64th Annual Conference on Magnetism and Magnetic Materials.

a) Corresponding author: p8qh258h@s.okayama-u.ac.jp

ABSTRACT

Manipulation of magnetic nanoparticles (MNP) by an external magnetic field has been widely studied in the fields of biotechnology and medicine for collecting and/or reacting biomaterials in the solutions. Here, dynamic behaviors of MNP in solution under changing gradient magnetic field were investigated using our newly developed laser transmission system (LTS) with a variable magnetic field manipulator. The manipulator consists of a moving permanent magnet placed beside the optical cell filled with MNP solution. A laser beam was focused on the cell and the transmitted laser beam was detected by a silicon photodiode, so that the localized concentration of the MNP at the focused area could be evaluated by the intensity of transmitted laser beam. In this study, the LTS was applied to evaluate dynamic behaviors of MNP in serum solution. Dispersion and aggregation of MNP in the solution were evaluated. While time evolution of dispersion depends on the serum concentration, the behavior during aggregation by the magnetic field was independent of the serum concentration. A series of measurements for zeta-potentials, distributions of particle size, and magnetization distributions was carried out to understand this difference in the behavior. The results indicated that a Brownian motion was main force to distribute the MNP in the solution; on the other hand, the magnetic force to the MNP mainly affected the behavior during aggregation of the MNP in the solution.

© 2020 Author(s). All article content, except where otherwise noted, is licensed under a Creative Commons Attribution (CC BY) license (<http://creativecommons.org/licenses/by/4.0/>). <https://doi.org/10.1063/1.5130167>

I. INTRODUCTION

Magnetic nanoparticles (MNP) have been widely studied in biology for manipulating biomaterials combined with MNP. MNP generally are a few nanometers in size, so that they show superparamagnetic. This superparamagnetic is considered to be one of good features of MNP for biological applications, because the magnetic moments of MNP rapidly relax by absence of external magnetic fields. Actually, a lot of emerging systems using MNP has been proposed and developed in biology and medicine: drug delivery using magnetic field gradients,^{1,2} magnetic particle imaging (MPI),³⁻⁶ and magnetic immunoassay (MIA).⁷⁻¹⁰ In this kind of applications, MNP are manipulated by magnetic field gradients, so

that it could be important to understand dynamic behaviors of MNP under exposure of magnetic field gradients. While static properties of MNP have been studied by many researchers using a scanning electron microscopy (SEM) and a transmission electron microscopy (TEM), dynamic behavior of the MNP has not been studied in detail. Also, in terms of “practical” applications of MNP, dynamic behaviors are supposed to depend on biological solvents; serum and body fluid.

In our group, a variable magnetic field manipulator with a permanent magnet placed beside a MNP solution cell has been developed for pre-treatment of magnetic immune assay, and we found that immune reaction of analytes with MNP beads could be promoting by our manipulator.¹¹ The theory of Brownian

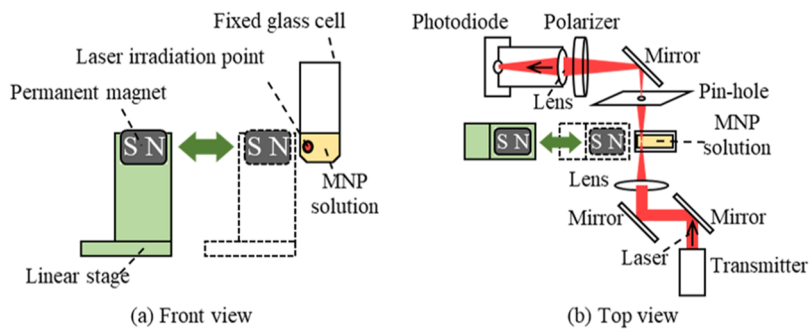


FIG. 1. System configuration: (a) Front view, and (b) Top view.

particle interaction with external magnetic force has been understood by classical electromagnetic laws.¹² However, there are few studies that experimentally evaluate the motion of MNP in actually biological solvents. Here, we have developed laser transmission system (LTS) with a variable magnetic field manipulator, which enable us to observe localized MNP concentration in the solutions while MNP are manipulating by the gradient of the magnetic field. Thus, we evaluate difference in the motion of MNP in different solutions using this system.

II. MEASUREMENT

A. Configuration

Fig. 1 (a) and (b) show the schematic front and top view of the developed LTS with the manipulator. A glass cell was used for sample container and the permanent magnet with the magnetic field density of 511 mT was placed beside the cell. The permanent magnet was mounted on a stepping motor-driven liner stage, so that the distance between the cell and the magnet, therefore, the magnetic field gradient across the cell, could be repeatedly changed. A neodymium magnet was used as the permanent magnet. The size of magnet was 15 cm times 10 cm times 10 cm, and the maximum energy product was between 342 and 366 kJ/m³. A laser beam produced by a conventional semiconductor laser was focused onto the cell with a spot size of 1 mm in diameter, while the internal dimension of glass cell was 10 mm in length, 2 mm in width, and 40 mm in height. The wavelength of the laser was ~635 nm. The laser beam transmitted through the cell was collimated by a convex lens and focused on a Si-pin-photodiode by an objective lens. The effective sensing area of the photodiode was 0.5 mm². A pinhole was mounted after collimation and a polarizer was applied in front of the photodiode; therefore, scattered laser beam by MNP could be suppressed. Thus, the transmittance of the cell, and the local concentration of the MNP, could be measured as the magnitude of the signal of the photodiode.

B. Sample preparation

Resovist (KYOWA CritiCare Co., Ltd., Tokyo) of 50 mg/mL was used as the MNP. The hydrodynamic diameter of Resovist and the MNP core diameter were 62.5 nm and 22.4 nm, respectively,¹³ and the volume fraction of MNP in Resovist was calculated with 0.0460 by assuming the particle as a sphere. Resovist was mixed with a serum-buffer solution of 200 μ L. The serum-buffer solution was prepared by mixing the serum and the 50-mM-HEPES

solution. The concentration in the serum-buffer solution was in the range of 0 to 5 v/v%. Resovist is a well-known contrast agent for liver, which consisted with nano-particles of iron oxide coated with carboxydextran.

III. RESULTS AND DISCUSSION

To observe the dynamic behaviors of dispersion of MNP for each sample, the transmittance was measured while the distance between the cell and the magnet increased from 4 mm to 49 mm. The speed of the magnet motion was at ~10 mm/s. The normalized transmittance as a function of time evolution was shown in Fig. 2 (a) and corresponding distance to the transmittance was plotted in Fig. 2 (b). The laser beam was focused close to the magnet in the cell as indicated in Fig. 1. Note that the time evolution of transmittance for 5%-serum was so slow that the transmittance reached to 1 is out of the time scale shown here. This saturation in the signal was at the time between 18 sec and 30 sec.

The transmittance was relatively low when the magnet was close to the cell, which indicated that the MNP were concentrated to the magnet side of the cell. By increasing the distance between the cell and the magnet, the transmittance gradually increased. This increment of the transmittance indicates that the MNP gradually

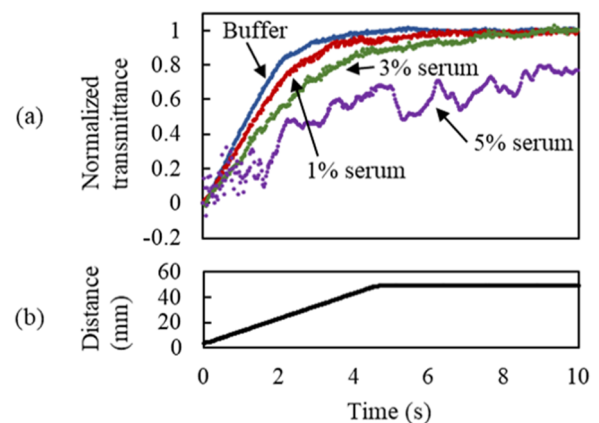


FIG. 2. Difference of diffusion lag by serum concentration: (a) The normalized transmittance as a function of time evolution, and (b) The distance between the magnet and the cell as a function of time evolution.

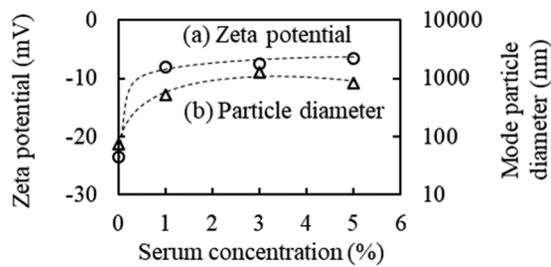


FIG. 3. Serum concentration dependence of status of MNP: (a) Zeta potential, and (b) Mode particle diameter.

diffused in the solution. For the 5%-serum solution, fluctuation in the transmittance was observed during the diffusion. This fluctuation might be caused because MNP aggregated and the particles with larger size passed across the laser beam.

We also found that the diffusion time increased by increasing the serum concentration in the buffer solutions. To understand the differences in the diffusion times for different serum concentrations, a series of measurements of the solutions was carried out on zeta-potentials, distributions of the particle size, and magnetic susceptibilities of the MNP in the serum solutions.

The zeta-potentials and distributions of particle size of MNP in the solutions were measured by an electrophoretic light scattering and a dynamic light scattering method, respectively, using a particle analysis system (Zetasizer nano ZS, Malvern Panalytical, United Kingdom). Fig. 3 (a) shows the zeta-potentials of the MNP, where the zeta potential is defined as the electric potential on the slipping plane where liquid flow occurs in the electric double layer.

The zeta potential of the MNP in the buffer solution was -23.5 mV while the zeta potentials were approximately -7 mV in the serum-solutions. The absolute values of zeta-potential for the serum-solution slightly decrease with increasing the serum concentration. Generally speaking, the particles show good dispersibility for the zeta-potential of around ± 25 mV. Therefore, the result suggests that, the MNP in the serum solutions easily aggregate while the MNP in the buffer solution maintains dispersibility.

The dynamic light scattering method was applied to the MNP as mentioned above, where scattering of the laser beam by the MNP

was observed and a fitting analysis using a diffusion coefficient was applied to the data. Thus, the distribution of the particle size could be evaluated. The diameters of the particles at the peak of distribution (mode particle diameters) are plotted in Fig. 3 (b). The diameter of Resovist in the buffer solution was 73.0 nm for this experiment. The serum solution mainly included larger particles of a few hundred nanometers in size in comparison with samples without serum.

The initial magnetization curves of the MNP in the solutions were measured using a low-temperature superconductor-superconducting (LTS-) quantum interference device (SQUID) magnetometer (MPMS3, Quantum Design, San Diego, USA) as shown in Fig. 4 (a). To reduce the magnetic signal from the solvent, differential signal was calculated by subtracting the signal of the sample containing only the solvent from the signal of the sample containing MNP. The MNP showed superparamagnetic properties and the magnetization slightly decreased with increasing the serum-concentration in the solutions. The magnetic moment distributions of the MNP in the solutions were calculated by fitting a Langevin model of superparamagnetism to the initial magnetization curves of MNP shown in Fig. 4 (a) and by applying the non-regularized inversion methods.¹⁴ The distributions are shown in Fig. 4 (b), the y axis represents the weighted intensity of magnetic moment corresponding to each core magnetic moment, and the “Intensity-weighted magnetic moment $n(m) \times m$ ” means the intensity of magnetic moment weighted corresponding number of the core. The magnetic moment distributions of the MNP mainly had two peaks, the first peaks with the magnitude of magnetic moments m of $1.1 \times 10^{-19} \text{ Am}^2$ and the second peaks with the magnitude of magnetic moments m of $2.4 \times 10^{-18} \text{ Am}^2$. The intrinsic saturation magnetization was determined to be $M_s = 300 \text{ kA/m}$ using the specific density of 5150 kg/m^3 for the MNP. The peaks around $m = 2.4 \times 10^{-18} \text{ Am}^2$ corresponded to an MNP core diameter of $d = 26.2 \text{ nm}$ by assuming $m = (\pi/6)d^3 M_s$.¹⁴ The calculated volume fraction of MNP in Resovist by our measurements was 0.0462, and almost same with the value as mentioned in the section II. The results in Fig. 4 (b) also indicate that the second peaks of the MNP shifted slightly in a direction of decreasing the magnitude of magnetic moments m with increasing the serum concentration. It could be that the particles were aggregated by increasing serum concentration, thus the magnetic moments weakened each other. It suggested

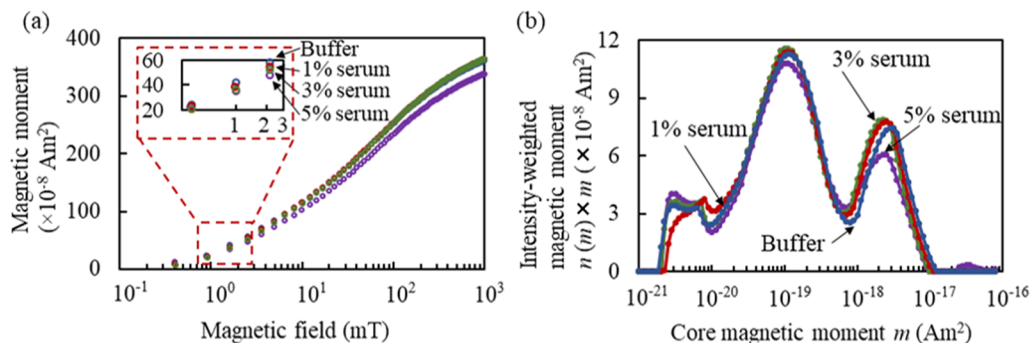


FIG. 4. Difference of magnetic characteristics of the sample by serum concentration: (a) Initial magnetization curves, and (b) Distributions of magnetic moment.

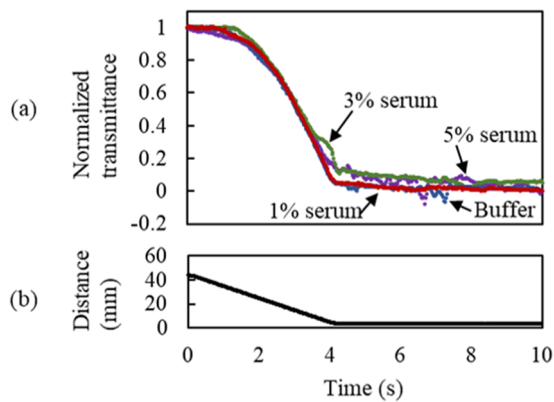


FIG. 5. Difference of aggregation lag by serum concentration: (a) The normalized transmittance as a function of time evolution, and (b) The distance between the magnet and the cell as a function of time evolution.

that the first peaks in the distributions were derived from original cores of the MNP, and the second peaks were derived from apparent large cores that may be attributed to other factors such as magnetic interactions between the nanoparticles and magnetic anisotropy.

Considering the series of measurements of MNP, decrease in the diffusion speed with increasing the serum concentration could be explained as following mechanism:

The fact that the magnetic moment distributions did not change by changing the serum concentration suggests that the magnetic forces to the MNP in the solutions received from the magnet might less effect on the MNP motions in Fig. 2, but a dispersion force of MNP effects on the MNP motion, which could change by the serum concentration. We have measured the serum concentration dependence of the viscosity in the concentration range between 0% and 50%. And as the result of interpolation of data, we found the change in the viscosity of the serum solution could be 2% in magnitude in the concentration range between 0% and 5%.¹⁵

Fig. 5 (a) and (b) show the time evolution of the transmittance of MNP in the solution and the distance between the cell and the magnet during the magnet approaching to the cell. Because the magnetic field density will increase in the cell, we expected that the MNP aggregate to the magnet side of the cell. The speed was at ~ 10 mm/s. Firstly, the MNP were diffused over the cell and gradually aggregated near the magnet. While the motion of MNP for diffusion largely depends on the serum concentration in the solution, the motion of MNP for aggregation was almost independent on the serum concentration. This result indicates that Brownian motion was dominated for the diffusion, the magnetic force mainly affected aggregation of MNP.

IV. SUMMARY

We have developed the LTS with the variable magnetic field manipulator to evaluate the behavior of MNP in the solutions. The series of measurements of zeta potentials, particle size distributions, and magnetizations of MNP was carried out to understand the observed behaviors. The results indicated that a Brownian motion was main force to distribute the MNP in the solution so that the motion depends on the viscosity. On the other hand, the magnetic force to the MNP mainly affected the behavior during aggregation of the MNP in the solution. These discussion could contribute to manipulate the MNP in actually biological tissues and bodies.

ACKNOWLEDGMENTS

This work was supported by a Grant-in-Aid for Scientific (S) (Grant No. JP15H05764) from the Japan Society for the Promotion of Science.

REFERENCES

- ¹F. Scherer, M. Anton, U. Schillinger, J. Henke, C. Bergemann, A. Kruger, B. Gansbacher, and C. Plank, *Gene Therapy* **9**, 102 (2002).
- ²S. D. Kong, J. Lee, S. Ramachandran, B. P. Eliceiri, V. I. Shubayev, R. Lal, and S. Jin, *J. Control. Release* **164**, 49 (2012).
- ³B. Gleich and J. Weizenecker, *Nature* **435**, 1214 (2005).
- ⁴T. Sasayama, Y. Tsujita, M. Morishita, M. Muta, T. Yoshida, and K. Enpuku, *J. Magn. Magn. Mater.* **427**, 144 (2017).
- ⁵R. A. Revia and M. Zhang, *Mater. Today* **19**, 157 (2016).
- ⁶E. U. Saritas, P. W. Goodwill, L. R. Croft, J. J. Konkle, K. Lu, B. Zheng, and S. M. Conolly, *Magn. Reson.* **229**, 116 (2013).
- ⁷S. Schrittwieser, B. Pelaz, W. J. Parak, S. L. Mozo, K. Soulantica, J. Dieckhoff, F. Ludwig, A. Guenther, A. Tschöpe, and J. Schotter, *Sensors* **16**, 828 (2016).
- ⁸K. Enpuku, Y. Ueoka, T. Sakakibara, M. Ura, T. Yoshida, T. Mizoguchi, and A. Kandori, *Appl. Phys. Express* **7**, 097001 (2014).
- ⁹K. Enpuku, M. Shibakura, Y. Arao, T. Mizoguchi, A. Kandori, M. Hara, and K. Tsukada, *Jpn. J. Appl. Phys.* **57**, 090309 (2018).
- ¹⁰T. Mizoguchi, A. Kandori, R. Kawabata, K. Ogata, T. Hato, A. Tsukamoto, S. Adachi, K. Tanabe, S. Tanaka, K. Tsukada, and K. Enpuku, *IEEE Trans. Appl. Supercond.* **26**, 1 (2016).
- ¹¹K. Tsukada, K. Tsunashima, K. Jinno, B. Hiramatsu, S. Takeuchi, K. Fujimoto, K. Sakai, T. Kiwa, and M. M. Saari, *IEEE Trans. Magn.* **55**, 1 (2019).
- ¹²R. Czopnik and P. Garbaczewski, *Phys. Rev. E* **63**, 021105 (2001).
- ¹³T. Yoshida, T. Nakamura, O. Higashi, and K. Enpuku, *Jpn. J. Appl. Phys.* **57**, 080302 (2018).
- ¹⁴M. M. Saari, K. Sakai, T. Kiwa, T. Sasayama, T. Yoshida, and K. Tsukada, *J. Appl. Phys.* **117**, 17B321 (2015).
- ¹⁵R. Isshiki, Y. Nakamura, S. Takeuchi, T. Hirata, K. Sakai, T. Kiwa, and K. Tsukada, *IEEE Trans. Appl. Supercond.* **28**, 1 (2018).